Fuel 291 (2021) 120074

Contents lists available at ScienceDirect

Fuel

journal homepage: www.elsevier.com/locate/fuel

Full Length Article

Characterization of the emission of particles larger than 10 nm in the exhaust of modern gasoline and CNG light duty vehicles

P. Dimopoulos Eggenschwiler *, D. Schreiber, K. Schröter

Empa, Swiss Federal Laboratories for Materials Science and Technology, Überlandstrasse 129, 8600 Dübendorf, Switzerland

ARTICLE INFO

Keywords:
PN larger than 10nm
PN emission
Gasoline light duty vehicles
CNG

ABSTRACT

Current particle number (PN) emission limits set by regulation, involve counted particles with a dimension >23 nm. The measurement procedure is specified and involves the dilution of the exhaust gas in a so-called constant volume sampling (CVS) device. Research efforts are concentrating in the further development of existing measurement techniques in order to capture smaller particles down to 10 nm, given their higher health threatening potential.

In the present study, six state of art, Euro 6, gasoline vehicles and in addition, one compressed natural gas (CNG) light duty vehicle, have been measured on the chassis dynamometer during different test cycles. Three particle sampling lines have been used, two in parallel at the CVS, counting particles >23 nm and 10 nm, and a third one directly at the tailpipe of the vehicle. The results allow a detailed evaluation of the emitted PNs. In addition, differences in the emissions patterns of the direct fuel injection (DI) and multi point port injection (MPI) gasoline vehicles could be identified. During cold starts, particles have been separated in distinctive size classes in order to obtain relevant number-size distributions.

Counting particles >10 nm resulted in roughly doubling the PN emissions in respect to those when counting particles >23 nm. This relation holds for all examined driving cycles. PNs measured at the CVS where significantly higher than at the tailpipe, especially when capturing also the smaller particles. The CVS could be identified contributing to the increase of the registered particle numbers during cycle parts with no or very low engine particle emissions.

Lowest PN emissions have been measured in combination with the CNG vehicle. The differences between DI and MPI gasoline vehicles have been significantly lower than expected from previous studies. While the MPI gasoline vehicles have been identified to emit more PN during cold start, the DI vehicles emit larger numbers during high engine loads. During cold starts, higher emissions of smallest particles have been evident.

The increased rated power to displacement ratio of modern engines, based on the current "downsizing" trend, shows a good correlation with the PN emissions.

1. Introduction

In recent years, legislation introduced particle number (PN) emission limits for diesel vehicles (light duty vehicles since 2011, heavy duty vehicles since 2014). The major effect, was the wide implementation of diesel particle filters (DPFs) in practically all new diesel vehicles. In parallel, several research investigations [1–4] reported high PN emissions of gasoline vehicles, in particular those utilizing direct injection (DI) for the fuel introduction in the combustion chamber. The more conventional multi point port injection (MPI) engines had been reported to have significantly lower PN emissions. A limit for the PN emissions of DI gasolines was introduced, effective from 2014. The PN limit though was higher than for diesel vehicles and only after September 2017, diesels and DI gasolines have to respect identical limits.

Abbreviations: CNG, Compressed natural gas; CPC, Condensation particle counter; CS, Catalytic stripper; CVS, Constant volume sampling; DI, Direct injection; DPF, Diesel particle filter; ECE, Economic commission for Europe, Urban driving cycle; ELPI, Electrical low pressure impactor; ET, Evaporation tube; EUDC, Extra-urban driving cycle; FMPS, Fast mobility particle sizer; GPF, Gasoline particle filter; IUFC, INRETS urbain fluide court cycle; MPI, Multi point port injection; NEDC, New European driving cycle; PDR, Power to displacement ratio; PEMS, Portable emissions measurement system; PFI, Port fuel injection; PMP, Particle measurement programme; PN, Particle number; PNC, Particle number counter; TWC, Three-way catalyst; VPR, Volatile particle remover; WLTC, Worldwide harmonized light vehicles test cycle.

* Corresponding author.

https://doi.org/10.1016/j.fuel.2020.120074
Received 6 October 2020; Received in revised form 7 December 2020; Accepted 22 December 2020
Available online 15 January 2021

Under these premises gasoline engine development followed several paths: On the one hand, focusing on the reduction of combustion particle formation has been pursued by tuning available combustion parameters, with most recent examples from Lee et al. and Yu et al. [5,6]. On the other hand, introducing a gasoline particulate filter (GPF), as most recently described by Ko et al. [7]. In parallel, the reduction of greenhouse gas emissions came into focus. Aiming for high efficiency lead to "downsizing" gasoline engines, i.e. to turbocharged engines with lower displacement and thus higher rated power per displacement ratios (PDRs). New DI and MPI gasoline engines followed this trend.

Also CNG (compressed natural gas) as a fuel for spark ignited engines has increased interest, because of its potential for greenhouse gas emission reduction. CNG is considered as a fuel with low particle formation properties, however, Alanen et al. reported a significant ultrafine particle formation and emission [8].

In general, the particles in the exhaust are considered to exhibit a trimodal number distribution characterized by the nucleation mode (20 nm), containing volatiles, droplets and smaller solid agglomerates, the accumulation mode (70 nm), consisting mainly of the solid agglomerates (soot) and condensed volatiles, and the coarse mode (500–1000 nm), consisting of larger agglomerates also formed during the path travelled by the exhaust, [4]. Most particles, by mass, reside in the accumulation mode, while by number sometimes the nucleation mode can dominate [9]. The forming and magnitude of a nucleation mode is depending on a series of engine, fuel and measurement/sampling parameters [3,4]. In order to avoid the variability of the nucleation mode, the European legislation introduced a PN measurement method based on the thermal pretreatment of the aerosol for measuring only the non-volatile fraction of the accumulation mode. This is achieved by passing the exhaust gas through a volatile particle remover (VPR) upstream the particle counter as well as by tuning the sensitivity of the particle counter accordingly. Thus, the particle number counters (PNC) to be used are counting 50% (cut-off size, 50%) of particles at 23 nm and > 90% at 41 nm, resulting in the possibility of solid particles, smaller than 23 nm, not being detected.

Morphological particle properties (size, shape, surface area, internal structure) of DI gasoline engines have been investigated by a limited number of studies. Barone et al. showed that primary particles were distributed in a range of 7 to 60 nm in diameter [10] which turned out to be somewhat wider than the size range of diesel particulates [11–14]. Gaddam et al. reported a narrower range (16–23 nm) [15]. In detailed TEM based investigations, Liati et al. reported primary particles between 4 and 55 nm in diameter, the majority being < 20 nm, while sub 20 nm particles have been more abundant during the more dynamic Worldwide harmonized light vehicles test cycle (WLTC) [14,16]. Monodisperse agglomerates comprising of very small (<20 nm), small (~25 nm) and larger (>35 nm) primary particles have been documented forming polydisperse but also monodisperse agglomerates. Most probably, polydisperse agglomerates consisted of particles formed during different operating conditions and later agglomerating in the exhaust duct. Liati et al. identified the cold start phase being the source of the larger primary particles [14]. All particles examined, however, exhibited lower degrees of crystallinity in respect to particles from diesel engines indicating higher reactivity. These results have been confirmed by direct measurements of the PN and size distribution by a series of investigations, the main results are accurately summarized by Giechaskiel et al. [3,4,17]. In addition, a number of recent studies, showing significant concentrations of particles < 23 nm, was summarized [3,4,17]. These particles are considered to be either metals from the lubricant, additives in the fuel or soot particles (heavy molecular hydrocarbons) formed in the combustion chamber. Based on measurements of the sub 23 nm fraction, the percentage of particles < 23 nm is around 20% for diesel vehicles and 30–60% for gasoline DIs, and low ambient temperatures (−7 °C) increase these percentages [4]. The measurement of the particle emissions of a CNG vehicle has underlined the importance of including ultrafine particles: the emission of particles of bigger sizes was low, while the ultrafine particles have been found to be significant [8]. A more recent investigation showed, that particles below 23 nm account for around 20% of the entire particle emissions (for LPG and CNG vehicles) [18].

Currently, it is widely accepted that PN measurements should be extended in order to include also particles down to 10 nm. In a series of investigations, Giechaskiel et al. assessed the influence of the PN counter tuning as well as the influence of the VPR on the measured sub 23 nm particles [17]. Changing the sensitivity of the PNCs for measuring particles up to 10 nm was found feasible; the influence of the VPR however, was significantly more complex. Losses inside the VPRs increase with decreasing particle sizes while pyrolysis and/or charring of semi-volatiles in the VPRs may lead to the formation of a solid nucleation mode artifact, i.e. hydrocarbons will be counted as solid particles. In addition, incomplete evaporation and re-nucleation of sulfuric acid may bias measurement results. In a recent investigation Giechaskiel et al. described in detail differences in PN emission measurements at the constant volume sampling (CVS) tunnel and the exhaust [19]. The problem became apparent after the light-duty vehicle reglementation was supplemented with on-road measurements using a Portable Emissions Measurement System (PEMS). The measurements were carried out stationary with identical PMP (particle measurement programme) compliant systems and two size ranges (>10 nm and > 23 nm) simultaneously at the exhaust and the CVS tunnel. The differences found for both size ranges were small (<15%), except for the cold start (up to 35%). In addition, a shift to larger particles from tailpipe to the CVS tunnel was found. The influence of the VPR on the measured particle emissions of a gasoline vehicle was also investigated by Ko et al. [7]. In this study the effect of a GPF (gasoline particle filter) and its emission reduction potential was also in focus.

The particulate emissions of modern SI vehicles with MPI have been shown to be significant by Czerwinski et al. [20]. In an extreme case, the PN-emissions were even in the range of Diesel vehicles (without DPF). It was also shown that the implementation of Gasoline Particle Filter (GPF) can reduce the particulate emissions below the current limits. In addition, it has been reported that with a catalytically coated DPF, not only particles but also CO, HC, NH3 and HCHO emission have been reduced. In parallel though, the GPF seemed to have a positive correlation with the emitted polycyclic aromatic hydrocarbons [X + 1]. A broad introduction of GPFs is expected to mitigate significantly PN emissions from gasolines. However, currently only DI gasoline vehicles are subjected to legislative particle emission limits. In relation to Czerwinski et al., Muñoz et al. assert, that MPI gasoline vehicles should have regulated particle limits [20,21].

The present study aims in providing a contribution towards all these open points. Seven state of art, Euro 6 light duty vehicles have been measured on the chassis dynamometer during the NEDC (New European driving cycle), WLTC (Worldwide harmonized light vehicles test cycle) and IUFC (INRETS urbain fluide court cycle). This sample group consisted of one CNG and six gasoline vehicles. Three particle sampling lines have been used, two in parallel at the CVS counting > 23 nm and > 10 nm particles, and a third one directly at the tailpipe. The results allow a detailed evaluation of the emitted PNs > 23 nm and > 10 nm. In addition, differences in the emission patterns of the DI and MPI gasoline vehicles could be quantified. A comparison to the PN emissions of older Euro 4 vehicles on the identical chassis dynamometer is also presented. During cold starts, particles have been separated in distinctive size classes in order to obtain relevant number-size distributions.

2. Methodology

2.1. Experimental setup

The vehicles have been examined on the chassis dynamometer of Empas laboratory. Exhaust from the tailpipe was collected and lead through a CVS (constant volume sampling) tunnel. Downstream the

CVS, a PMP compliant particle counting system, comprising of VPR (volatile particle remover) and a condensation particle counter (CPC) with a sensitivity for counting 50% of the particles with a size of 23 nm (Fig. 1, system Empa VPR1 PMP), was installed. The VPR of this system was an evaporation tube (ET) operated at a temperature of 350 °C.

An additional counting system (Fig. 1, system: AVL 498-cs) with a counting efficiency of 50% of 10 nm particles was connected with a flow-splitter in parallel to the PMP compliant counting system. The system from AVL was specially developed for sub 23 nm particle counting and was equipped with an integrated Catalytic Stripper (CS) as a VPR. The CS removes the volatile particles more efficiently, but has also higher solid particle losses [22].

At the tailpipe a third (Empa, VPR2), counting system was directly connected, in order to assess the influence of the CVS. The

CPC at this sampling location had a counting efficiency of 50% for 10 nm particles. For additional information on the transient PN size distribution a fast mobility particle sizer (FMPS, from TSI) was connected in parallel to the CPC of the third counting system. The particle size spectrum, measured at the FMPS, was separated in three size classes, ultrafine (10.8–22 nm), fine (25–70 nm) and coarse (81–523 nm). This size class separation was considered as reasonable and accepted as a result only if the sum of the three classes resulted in particulate numbers approximately equal to those measured by the parallel CPC. As a quantification limit for the FMPS, a PN of 4×10^9 /s was considered as reliable. Lower values have not been taken into account. Because of this limitation, PNs measured in the size class of 10.8–22 nm were not always complete and the trends not always plausible.

In addition, two different electrostatic particle sampling systems were connected downstream of a heated dilution tube which in turn was connected to the tail pipe. One of them was a total particle sampler and the other a combination of an electrical low pressure impactor (ELPI) and an electrostatic sampling system as described by Liati et al. [16]. With this configuration, the second system samples particles in the range of the ELPI back-up stage (up to < 30 nm). To increase the number of charged particles the ion trap of the ELPI was not in operation [23].

2.2. Examined vehicles

One CNG (compressed natural gas) and six gasoline vehicles have been examined in this study, all of them certified according to Euro 6b regulations. These vehicles were all serial production vehicles and have been borrowed for the measurements from their regular users. They were newer than 7 years, were equipped with a three-way catalyst (TWC) as exhaust after treatment and had <100′000 km total driven range. Prior to the measurements, the vehicles have been technically examined and no defects have been found. The rated PDR (power to displacement ratio) of the vehicles' engines was one of the criteria for their selection. Vehicle PB6-01 had an engine with a very high rated PDR, in the range of engines for racing vehicles. Vehicles PB6(02–04) had high PDR resembling the current trend of downsized engines for achieving high energetic efficiency and low fuel consumption. Vehicles PB6-05 and PB6-06 had engines of only moderate PDR, typical for conventional gasoline powertrains.

Table 1 summarizes the main technical characteristics of the examined vehicles. None of the measured vehicles was equipped with a GPF (gasoline particle filter). An additional distinction is the fuel injection system. Some of the gasoline engines had DI (direct fuel injection) in the cylinder, while the others had a more conventional MPI (multi point port injection). The DI gasoline engines are known to have higher particle emissions than the MPIs [2]. In addition, CNG vehicles are expected to have the lowest particle emissions, given that the gaseous fuel is less prone to form dense fuel films on walls in and around the cylinders. The CNG engine used in this study was equipped with a multi point injection in the manifold.

2.3. Driving cycles

The vehicles have been tested, using different international established driving cycles. Every vehicle was examined during the old, NEDC (new European driving cycle), and the new certification, WLTC (Worldwide harmonized light vehicles test cycle). For cold start analysis, the IUFC (INRETS urbain fluide court cycle) was applied. The driving cycle velocity profiles, with specific indication of each cycle phase, are shown in the following graphs (Figs. 2–4).

A cold start cycle (First parts in Figs. 2–4) is started with a cold engine having the ambient temperature, meaning it can be performed at different temperatures. In this study the cold start cycles have been performed at 23 °C. The emissions of each vehicle were measured once for every driving cycle.

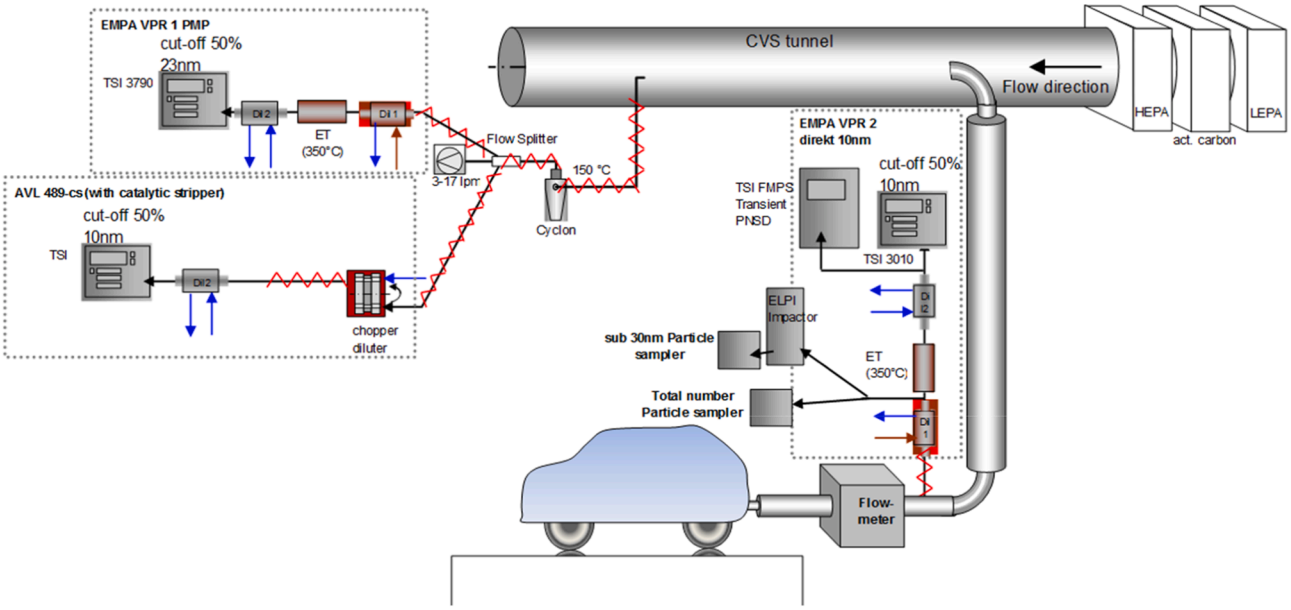

Fig. 1. Schematic of the measurement setup for the PN measurements.

Table 1
Specifications of the examined vehicles.

Vehicle label	PB6-01	PB6-02	PB6-03	PB6-04	PB6-05	PB6-06	PCNG6-01
Fuel type	Gasoline	Gasoline	Gasoline	Gasoline	Gasoline	Gasoline	CNG
European emission limit standard	Euro 6b	Euro 6b	Euro 6b	Euro 6b	Euro 6b	Euro 6b	Euro 6b
Power to displacement ratio (PDR)	111.4 kW/l	90.1 kW/l	91.4 kW/l	88.0 kW/l	73.4 kW/l	55.5 kW/l	58.1 kW/l
Fuel injection system	Direct Inj.	Direct Inj.	Multi Point Inj.	Multi Point Inj.	Multi Point Inj.	Multi Inj.	Multi Point Inj.
Exhaust after treatment	TWC	TWC	TWC	TWC	TWC	TWC	TWC

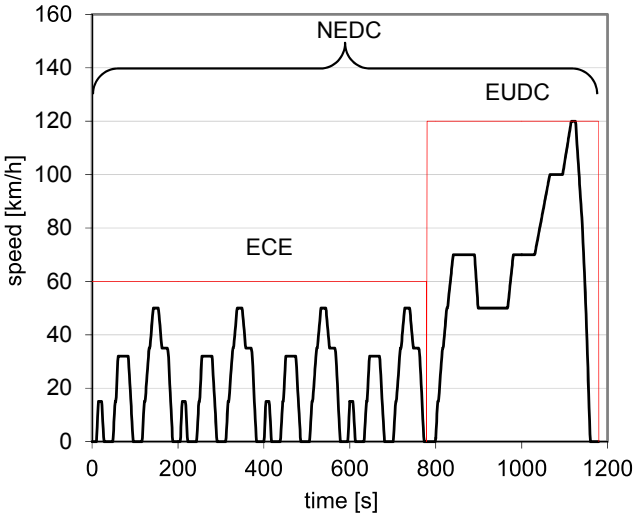

Fig. 2. NEDC, new European driving cycle, including a cold start at 23 °C.

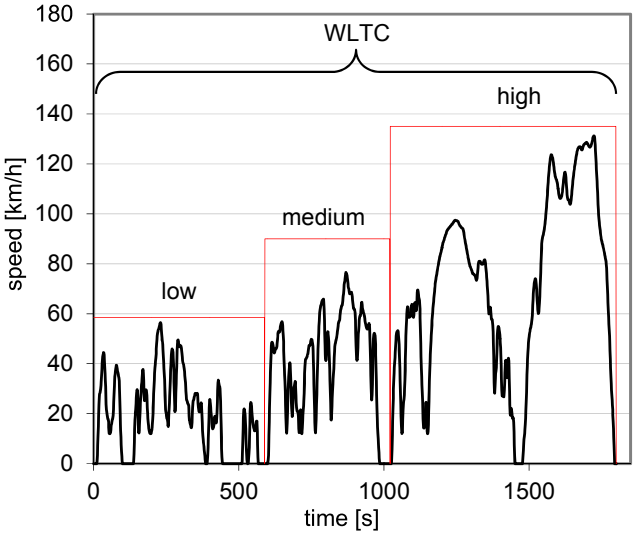

Fig. 3. WLTC, Worldwide harmonized light duty test cycle, including a cold start at 23 °C.

3. Results and discussion

3.1. Comparison of PN emissions with detected particle sizes > 10 nm and > 23 nm

Fig. 5 shows the emissions of the tested gasoline vehicles at the different parts (ECE, Urban driving cycle and EUDC, Extra-urban driving cycle), as well as the entire NEDC, acquired in parallel by two different sampling lines downstream the CVS (CVS > 10 nm and CVS > 23 nm) and one at the tail pipe (Tail pipe > 10 nm). In addition, the Euro 6b (6×10^{12} /km), 6c and 6d (6×10^{11} /km) PN emission limits are marked.

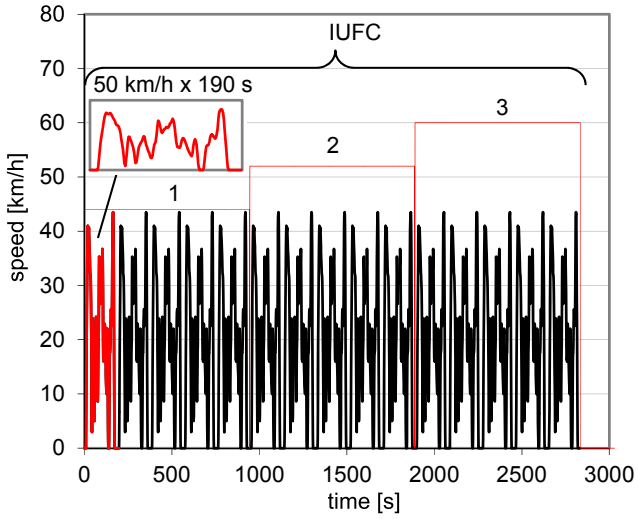

Fig. 4. IUFC, INRETS urbain fluide court cycle, a suitable cycle for studying cold start emissions.

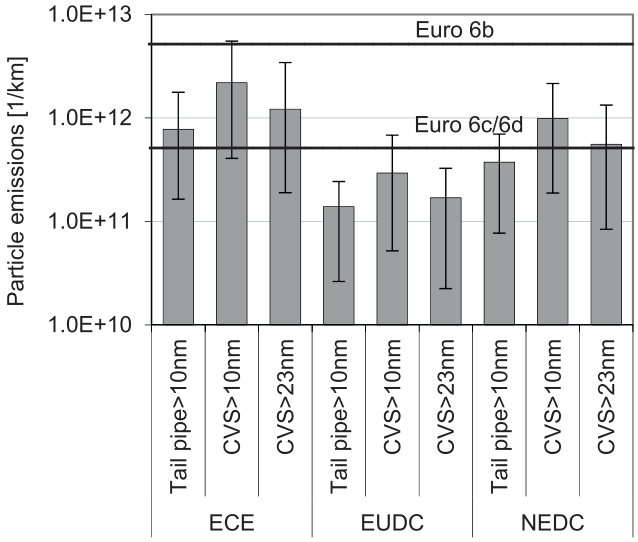

Fig. 5. Average PN emissions of the gasoline vehicles, measured by the three different sampling systems during the NEDC, with indication of minimum and maximum measured emissions.

All vehicles respect the Euro 6b emission limit, even when particles >10 nm are measured. After all, the vehicles have been homologated according to this limit. In parallel, average PN emissions are close to the Euro 6c limit with only two of the vehicles clearly exceeding it. Based on the established PN measurement system, detecting particles > 23 nm downstream the CVS, the average Euro 6 gasoline vehicle emits 5.5×10^{11} /km particles at the NEDC, including a cold start (at 23 °C). However, highest PN emissions have been measured in the first part of the cycle (the ECE) and are due to the cold start (analysis in more detail

in Subsection 3.5). The PN counted by the second system (CVS > 10 nm) has been roughly twice as high in respect to counting the particles bigger than 23 nm in the same location, after the CVS. Interestingly, counting particles > 10 nm at the tailpipe resulted in the lowest PNs. This raises the question whether the higher PNs downstream the CVS (in respect to the tailpipe measurements) are emitted by the engine or whether they have been in the CVS from previous measurements (a CVS artefact). Some additional arguments in this point follow in the discussion in Subsection 3.2.

The NEDC was the prescribed cycle for the homologation of the measured vehicles. In the meantime, it is replaced by the WLTC, being more representative for everyday driving. The PN emissions over this cycle are shown in Fig. 6. The average Euro 6 gasoline vehicle is emitting 1.6 times more particles over the WLTC in respect to the NEDC. Interestingly, all other relations, as reported for the NEDC, are also holding for the WLTC:

- PNs counted at the CVS with particles >10 nm are roughly two times higher than PNs including particles >23 nm at the same location.
- PNs at the tailpipe (even > 10 nm) are lower than at the CVS
- Highest particle emissions are measured at the first cycle part including the cold start.

3.2. Influence of the PN sampling location

The PNs with a size > 10 nm counted at the CVS are 2.5 times higher in respect to the PNs detected at the tailpipe with > 10 nm, for the NEDC (3.74×10^{11} /km) and the WLTC (6.34×10^{11} /km).

Within the experimental setup, the PNs measured directly at the tailpipe are in general the lowest. These observations evidence that the CVS and associated transfer pipes maybe sources of additional small particles, which are not attributable to the engine. The high PNs after the CVS can be effects of a particle formation during the flow through the CVS. A more detailed analysis of individual vehicle measurements revealed a delayed decline of PNs for both CVS located systems in respect to the tailpipe system in cycle phases with fuel cut-off, where actually the PN emissions are expected to decline sharply. Fig. 7 shows a example of this behavior of the measured PNs during the NEDC of a MPI gasoline vehicles with the corresponding driving speed (v Dyno). The difference in particle emissions between the sampling point at the CVS and the one at the tailpipe during fuel cut-off phases is marked.

These discrepancies can be attributed either to storage and release

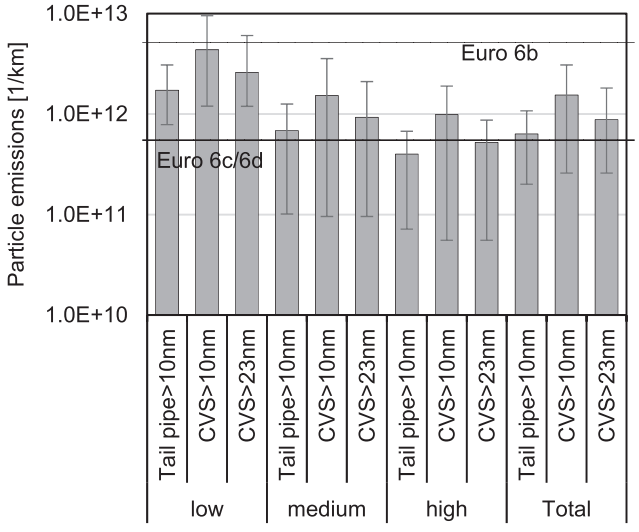

Fig. 6. Average PN emissions of the gasoline vehicles, measured by the three different sampling systems during the WLTC, with indication of minimum and maximum measured emissions.

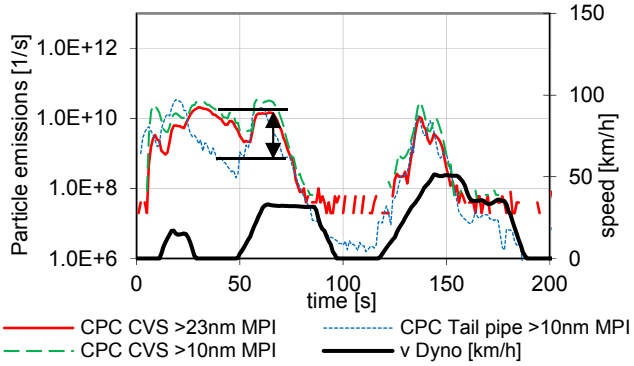

Fig. 7. PN emissions one gasoline MPI vehicle as measured by the three different sampling systems during the NEDC.

effects of the CVS or to gas run time differences from the different sampling locations to the instruments. The longer time between the emission and the detection leads to the possibility of agglomeration effects of very small particles, forming detectable particles of > 10 nm inside and after the CVS. In addition, Fig. 7 shows that high PNs after the CVS, in the intervals where these are expected to have decreased, are more pronounced for the sampling of particles > 10 nm. It is worth raising the issue, whether sampling at the CVS is appropriate when counting smallest particle sizes. This point has also been mentioned recently by Giechaskiel et al. [19].

3.3. Comparisons of PN emissions of Euro 4 and Euro 6 gasoline vehicles

Using data from a previous, own, study on Euro 4 vehicle particle emissions, [2] a comparison to the corresponding emissions of the modern Euro 6 vehicles can be obtained. The Euro 4 emissions shown in Fig. 8, were measured at the CVS tunnel with a CPC, counting all particles > 7 nm. Thus, the only acceptable comparison of Euro 6 particle emissions to these results, is based on the particle emissions measured

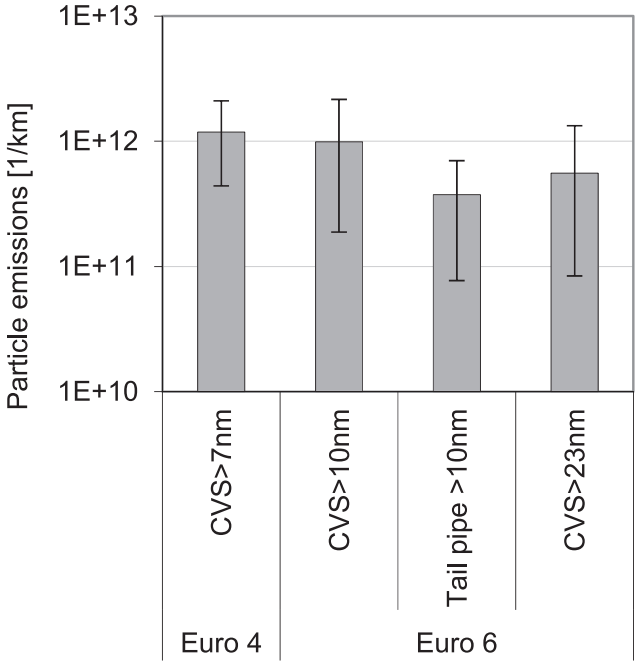

Fig. 8. Comparison of average NEDC PN emissions of Euro 4 [2] and Euro 6 gasoline vehicles. The bars show the average PN emissions of all tested vehicles of different injection types, while the minimum and maximum measured emissions were in the given variation range.

downstream the CVS, detecting particles > 10 nm. The emitted particles by the Euro 4 and Euro 6 vehicles are very similar in their numbers. What should be taken into account though is, that the measured Euro 4 vehicles had a significantly lower rated PDR (in average around 52 kW/l) while the average measured Euro 6 vehicle had 85 kW/l. In Subsection 3.6 we focus on the influence of the rated power density of the engine on the emitted particles.

3.4. Influence of the gasoline injection system on PN emissions, comparison to a CNG vehicle

Fig. 9 shows a direct comparison of the PN emissions of the gasoline vehicles, having separate averages for the vehicles with DI and MPI fuel injection system, during the NEDC. In addition, the PN emissions of one single CNG powered vehicle (with port fuel injection, i.e. no DI) are also included. The sampling location was directly at the tail pipe and all particles > 10 nm have been counted.

Clearly, the CNG vehicle has the lowest PN emissions, with over one order of magnitude lower than the gasoline vehicles. On the other hand, the differences among the two gasoline vehicle classes are rather small. MPIs emit more particles in the first cycle part (ECE, including the cold start and lower engine loads), while DIs have higher PN emissions than MPIs in the second part, associated with higher engine loads. The resulting entire NEDC PN emissions are very similar. This is rather surprising, given the recent focus of literature and legislation on the PN emissions of DI gasoline vehicles.

The higher PN emissions of the DIs in the cycle parts with higher loads can be attributed to poor fuel air mixing as well as to increasing build-up of liquid fuel films on cylinder walls and pistons. With increasing load, the amount of fuel and the injection duration increase. Therefore, a significant part of the fuel has to be injected in the late stages of the intake stroke with decreasing time available for a complete homogenization of the cylinder charge. In the previous study with Euro 4 vehicles, [2] DI PN emissions, of at least one order of magnitude, higher in respect to the MPIs have been reported.

Fig. 10 shows the emitted PNs during the NEDC from the 2017 study (Euro 4) [2] comparing them to the recent results for DIs and MPIs (Euro 6) at different sampling locations.

DI gasoline PN emissions are significantly lower regarding Euro 6 vehicles in respect to the Euro 4 DI gasoline engines. For MPIs, the corresponding results of the Euro 6 vehicle measurements (CVS > 10 nm) indicate an increase of the average emissions, but stay in total in the same range, compared to the Euro 4 results.

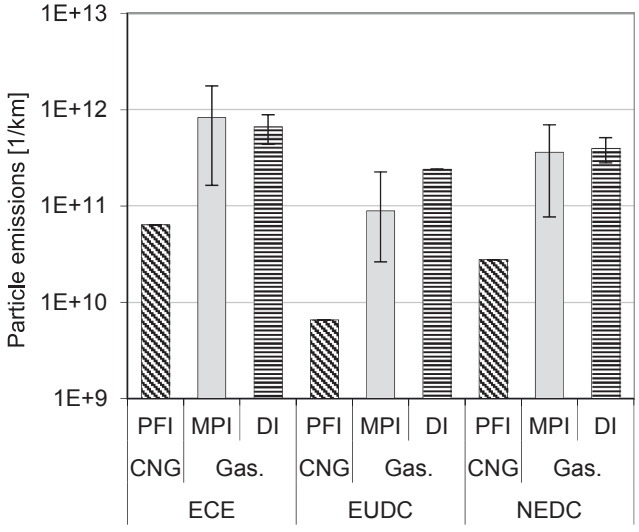

Fig. 9. PN (>10 nm) emissions, detected at the tailpipe, of the six gasoline vehicles and one CNG vehicle during the NEDC, with indication of minimum and maximum measured emissions of each vehicle class.

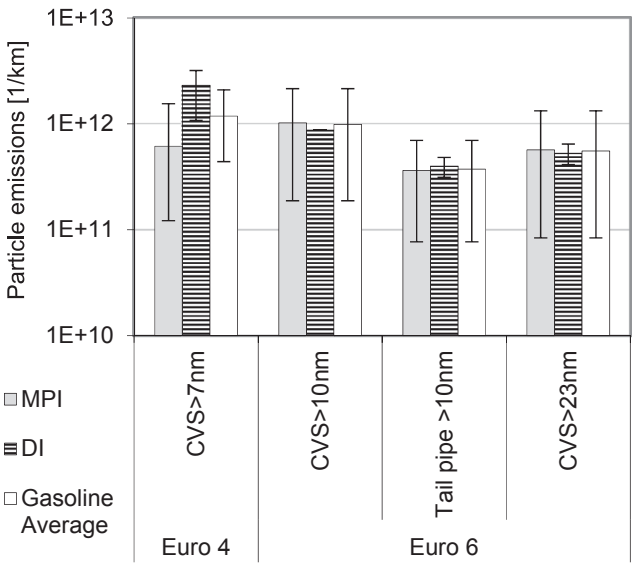

Fig. 10. Comparison of NEDC PN emissions of Euro 4 [2] and Euro 6 gasoline vehicles with different fuel injection systems, with indication of minimum and maximum measured emissions of each vehicle class.

3.5. Relevance of a cold start for PN emissions

The amount of cold start emissions can be evaluated with the IUFC. Fig. 11 shows the PN emission of the three repetitions and the total average emissions of the IUFC at 23 °C. Within this experiment, the particles > 10 nm and > 23 nm were detected at the tailpipe and downstream the CVS respectively. The IUFC is suitable in order to demonstrate the influence of the engines warm-up on the emissions.

The emissions of both, DIs and MPIs, during the first sequence are significantly higher than the emissions of the second or third part. The PNs are in average twelve times higher in the first sequence (e.g. at the tailpipe, > 10 nm: 5.46×10^{12} /km), than in the second and roughly in the third (e.g. at the tailpipe, > 10 nm: part 2: 6.05×10^{11} /km; part 3: 4.71×10^{11} /km).

Between the second and third IUFC sequence, the decrease of the PN

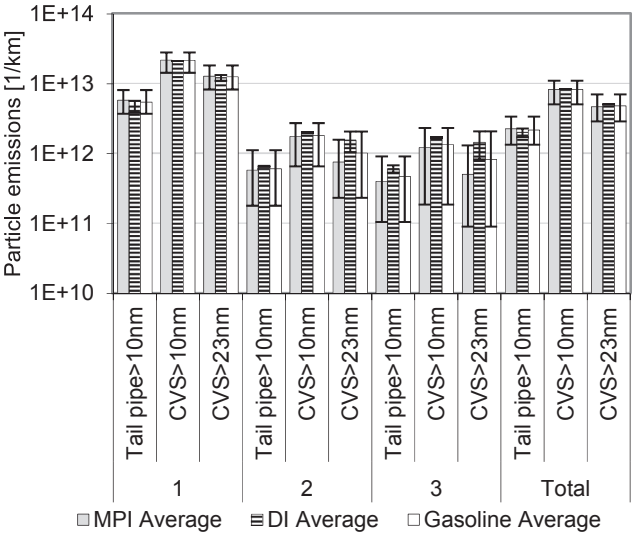

Fig. 11. IUFC phases (1, 2, 3) and total cycle average PN emissions, measured with the three sampling systems, with indication of minimum and maximum measured emissions of each vehicle class.

emissions is modest, for DIs and MPIs. The differences among the measuring sites are similar as previously discussed (Sections 3.1 and 3.2). While the emissions at the tailpipe are the lowest, the ones after the CVS with sizes > 10 nm are higher than emissions of particles > 23 nm (after the CVS).

The influence of the different injection system is more clearly pronounced in the IUFC. For cold starts, the MPIs have higher or similar emissions as the DIs. With warmer engines, MPIs emissions decrease dramatically. This result is in line with the one discussed at Section 3.4, with Fig. 9. An explanation for the high particle emissions of the MPIs during the cold start are either increased tendency to form liquid films in the engine ports and valves or active catalyst heating strategies that are used in state of the art gasoline engines (or even both). Active catalyst heating strategies are based on late ignition timing and cylinder scavenging. Thus exploiting the positive pressure difference that occurs between the intake and the exhaust channel during parts of the gas exchange stroke, mainly when the piston is around the bottom dead center [24]. Should the opening time of intake and exhaust valves overlap, then fresh gas pushes the remaining burned gas out of the cylinder to the exhaust channel. This is heating up the catalyst, while giving an additional boost to the turbine. The disadvantage (apart from the higher fuel consumption) of these strategies lies in the high particulate emissions, predominantly generated by very slow late combustion (because of the late ignition timing) taking place under very low turbulence levels. For counteracting and restricting particulate emissions, some gasoline DIs use an additional, small, late fuel injection (enhancing turbulence, mixing and combustion rates late in the cycle, [25,26]).

3.6. PN size distribution at cold starts

Fig. 12 and 13 show size distributions of the PNs emitted during the cold start of the WLTC for one DI and one MPI gasoline vehicle respectively. The measurement system is described in detail in Section 2.1. In the very beginning of the cold start, DI and MPI, engines emit small and mid-sized particles only. After approx. the first 10 s, big particles are dominant and the number of small particles decrease. After roughly the first 20 s, the most particles are in the mid-size (25–70 nm) class. The smallest particles (10.8–22 nm) are the second abundant class while the bigger particles are one order of magnitude less. During the following time of the test procedures, the total PN decreases and because of the separation into three size classes, the PN is fractioned. This leads to a PN lower than the measurement accuracy in each class and therefore cannot be analyzed or shown.

The measurement accuracy of the system is around 4×10^9 /s (dashed red line). Concentrations below this limit are also detectable, but the results are not reliable and therefore have not been taken into account. After the first 100 s of the driving cycle, the PN of each size class, as well as the total, lies below this limit. Within roughly the first 50 s, the detection with the FMPS was feasible and delivered reliable particle size distributions. In this stage, the sum of the particle size classes, detected with the FMPS (violet line) resembles quite accurately the total PN emissions, measured separately at the tailpipe with sizes > 10 nm (black line). There is no reason to assume that the particle size distribution later in time does not continue to have a high fraction of small particles.

3.7. Influence of the rated engine power density on PN emissions

To compare the four different MPI vehicles, Fig. 14 shows the time resolved particle emissions, as measured at the CVS during the first 800 s of the NEDC. The particles > 23 nm are taken into consideration. The high peaks in the beginning of the cycle are typical for acceleration phases during the cold start. The trends of all four vehicles are comparable. The magnitudes of the peaks, however, differ significantly. Interestingly, the highest peaks, as well as the highest integral value over the entire cycle, (in respect to all the other MPIs) were from MPI vehicle No. 4. The layout of the engine of this vehicle was the one following most closely the current “downsizing” design imperatives, having small displacement and only two cylinders. Downsizing of engines aims for increased efficiency by reducing the engine displacement while in parallel maintaining (rated) power at the levels of an engine of a larger size. This can only be achieved by a matching turbocharger layout. The turbocharger is capable of providing high levels of air to the engine which allows also high levels of fuel amounts to be injected (all examined engines rely on stoichiometric fuel air mixing). The engine geometrical features (intake channels, valves, cylinders, pistons) cannot be increased accordingly. Inevitably, liquid fuel films on channel, cylinder and piston surfaces increase, deteriorating fuel–air mixing and increasing particle emissions. As a measure of the ”downsizing” degree of an engine, the ratio of the rated PDR is usually considered. MPI vehicle No. 4 had a ratio of about 90 kW/l, which is considered as sufficiently high for MPIs. Interestingly, MPI vehicle No. 3, having lower but after all very similar particle emission characteristics, had a similar rated PDR, but was equipped with a four cylinder engine, i.e. less restricted surfaces. MPI vehicles No. 5 and 6 had much lower particle emissions as well as much lower rated PDRs (75 and 55 kW/l respectively).

Fig. 15 shows the time resolved particle emissions of the two DI vehicles as measured at the CVS in the last approx. 400 s of the NEDC. Here again particles > 23 nm are observed. Striking is, that the two vehicles have strongly differing particle emission characteristics. Apart from the acceleration phases, DI vehicle No. 2 displays significantly high particle emissions during all high load periods. Interestingly, this was the vehicle with an unusual high PDR, 111 kW/l. The engine layout is therefore aiming to exceptional high performance for a racing type street vehicle. DI vehicle No. 1 had a moderate rated PDR for DIs of 90 kW/l.

In addition to the injection type specific particle emission characteristics and in respect to Schreiber et al., it was observed that the engine with the highest rated PDR was the highest PN emitter, by far [2]. In parallel, the engine with the lowest rated PDR had the lowest particle emissions. Fig. 16 displays the PN emissions during all relevant cycle parts of all measured gasoline vehicles over the rated PDR (NEDC, top; WLTC, bottom).

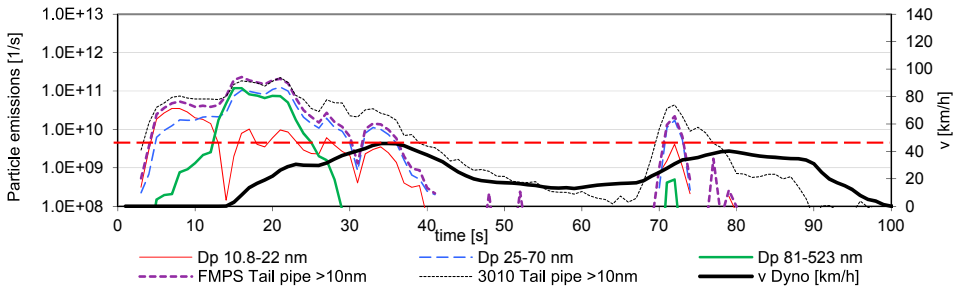

Fig. 12. PN size distribution of one DI gasoline vehicle during the cold start of a WLTC at 23 °C, measured at the tailpipe.

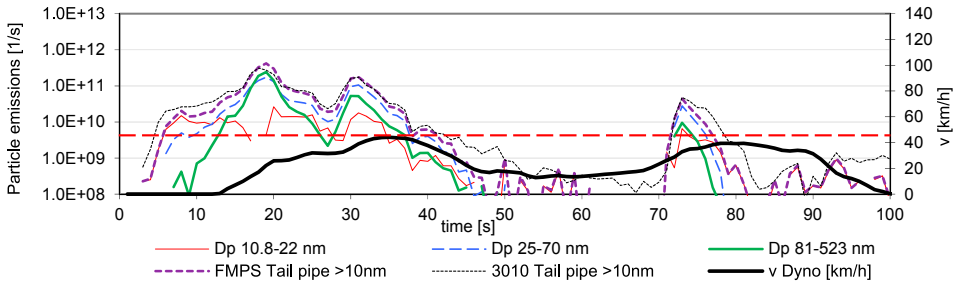

Fig. 13. PN size distribution of one MPI gasoline vehicle during the cold start of a WLTC at 23 °C, measured at the tailpipe.

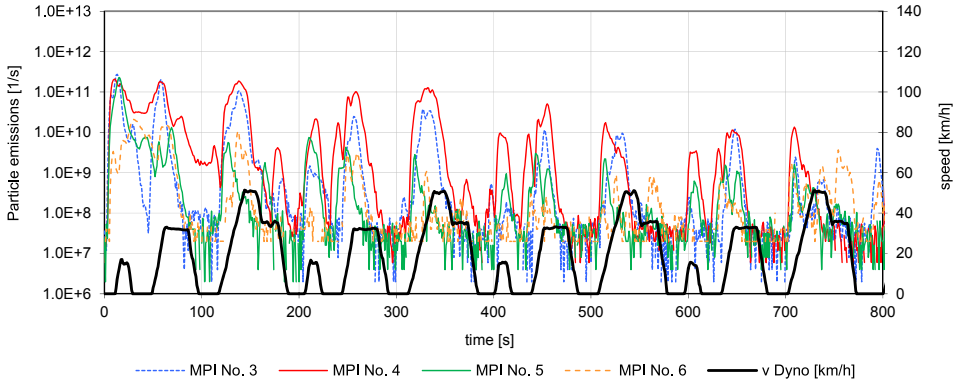

Fig. 14. PN emissions (>23 nm) of four MPI vehicles during the first part of a NEDC at 23 °C, measured at the CVS.

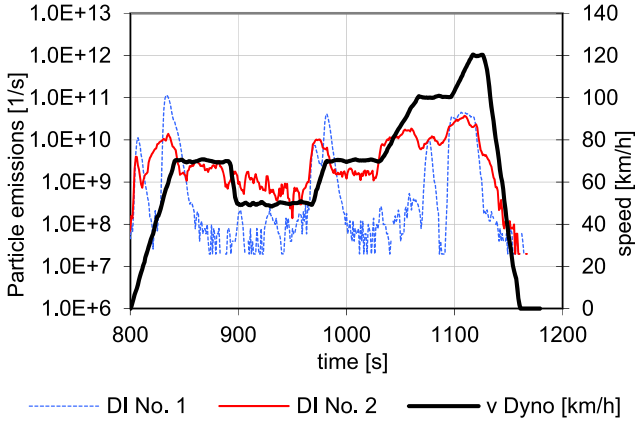

Fig. 15. Time resolved particle emissions (>23 nm) of two DI gasoline vehicles in the late part of the NEDC, measured at the CVS.

The PN emissions seem strongly correlated with the rated PDR in all cycle parts with warm engines. These parts are EUDC in the NEDC (Fig. 16, top) and "medium" and "high" in the WLTC (Fig. 16, bottom). In these cycle phases, the particle emissions are exponentially proportional to the PDR with an exponent of about 0.05. The injection type does not influence this correlation, as there are no significant differences between MPI and DIs. In the range of high PDRs, the PN emissions can deviate from the exponential function. In the cycle parts with a cold start (ECE of NEDC and "low" part of WLTC), there is only a weak correlation of the PN and the PDR. The exponential factors for these cycle parts are 0.005 (WLTC) and 0.04 (NEDC) and these are only reliable for lower PDRs. These correlations in cold engine cycle parts between PDR and PN emissions are currently not applicable because of the small sample group and need to be examined furthermore. For the small survey group of six vehicles, the dependencies in warm engine cycle parts are actually existing and reliable. This shows a strong impact of increasing the PDR as a downsizing method on the PN emissions. Additional vehicle investigations are necessary for verifying this hypothesis. Based on the reasoning for the correlation of the particle emissions with the rated PDR, offered further above, it can be expected that the correlation (with modified coefficients) may hold for a large number of gasoline vehicles.

4. Conclusions

In this study, the particle number (PN) emissions of six typical gasoline and one CNG powered vehicles, all homologated according to the Euro 6b emissions limits, have been studied in detail. The general results can be summarized as follows:

- The average PN emissions (particles >23 nm) of the gasoline vehicles over the NEDC, measured as prescribed by the PMP protocol downstream a CVS, is 5.5×10^{11} /km.
- The CNG vehicle measured, had significantly lower PNs of more than one order of magnitude (3.5×10^{10} /km) compared to the gasoline vehicles.
- Measuring all particles >10 nm in the same sampling position (downstream the CVS), results in roughly doubling the emission value.
- Measuring PNs directly at the tailpipe results in significantly lower PN numbers (2.5 times lower), compared to the PNs at the CVS.
- The PN emissions during the WLTC, are roughly 1.6 times higher than during the NEDC.
- The above conclusions concerning the NEDC hold similarly also for the WLTC and other cycles.

PNs measured directly at the tailpipe have been always significantly lower in respects to those at the CVS. The analysis of discrete cycle parts with fuel cut-off phases shows, that the PNs at the CVS do not decline as fast as those at the tailpipe, following the decline of the engine load. This effect is stronger for PNs > 10 nm in respect to those for PNs > 23 nm. A series of such observations raise the issue whether the CVS is a suitable system and whether the artefacts introduced by it are too high for

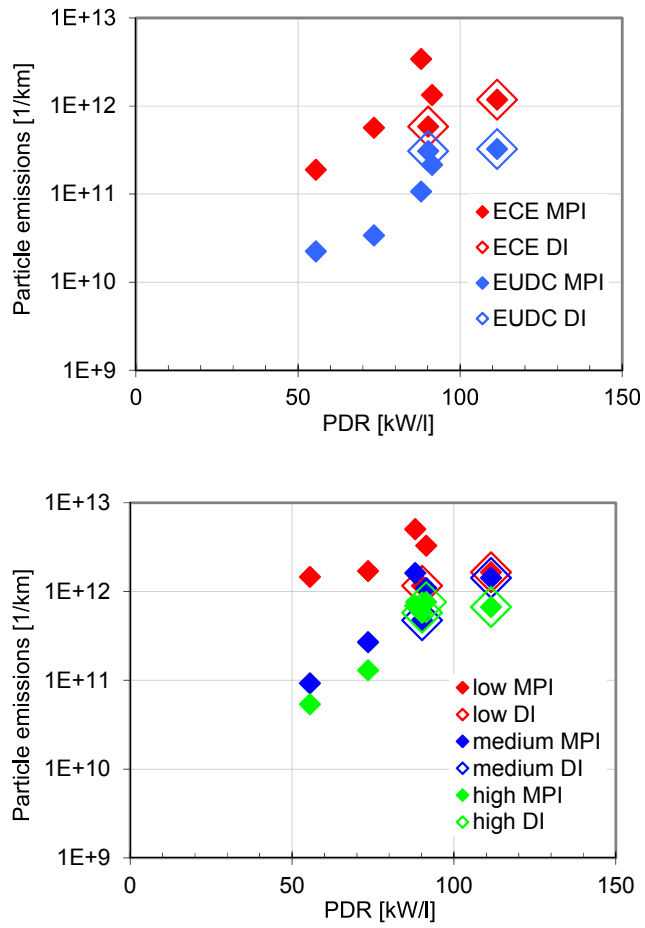

Fig. 16. PN emissions of the gasoline vehicles during the two parts of the NEDC (top), and during the three parts of the WLTC (bottom) over the rated PDR of each engine.

quantifying small particles. We agree with the conclusion in [19] that tail pipe sampling is not only possible but it can give more representative emissions, in particular when PN > 10 nm are in focus.

The comparison of the PN emissions of Euro 4 and Euro 6 vehicles showed:

- Euro 4 and 6 vehicle PN emissions are on a very similar level.
- The average rated power density of the Euro 6 vehicles was around 25% higher in respect to the Euro 4 vehicles.
- Taking into account the PNs (>10 nm), the DI Euro 6 vehicles have lower emissions than the Euro 4 DI vehicles, while the MPI Euro 6 vehicles have a similar range of particle emissions as the Euro 4 MPIs.

Differences of the PN emissions among the gasoline vehicles relying on DI and on MPI were very small, lower than expected.

- MPIs emitted more particles during cold starts and less under high loads.
- DIs emitted more particles under high loads and less during cold starts.
- The PN emission patterns of the different MPI vehicles were very similar during the test cycles, only the magnitude of the peaks differed from vehicle to vehicle.
- The PN emission patterns of the different DIs were varying, not only in magnitude but also in overall behavior.
- In the cycle parts with warm engines, PN emissions show a dependence on the rated power to displacement ratio.

During cold starts, all examined vehicles emit at least one order of magnitude more particles than during normal operation. In the first seconds after a cold start, all measured vehicles emit predominantly ultrafine and fine particles. Some 10 s later, the emissions of coarser particles starts.

However, more, similar investigations are needed in order to verify the conclusions of this work over a larger number of vehicles.

CRediT authorship contribution statement

P. Dimopouls Eggenschwiler: Conceptualization, Methodology, Funding acquisition, Project administration, Resources, Supervision, Writing - original draft. **D. Schreiber:** Investigation, Methodology, Formal analysis, Software. **K. Schröter:** Data curation, Validation, Writing - review & editing.

Declaration of Competing Interest

The authors declare that they have no known competing financial interests or personal relationships that could have appeared to influence the work reported in this paper.

Acknowledgements

The authors gratefully acknowledge the Swiss federal Office for Environment for the project “Modellierung und Validierung des Katalysatorverhaltens bei Kaltstart und im Gesamtzyklus”, contract no 15.0002.PJ / S122-1359 as well as the project “Sub 30 nm Partikel Untersuchung an Diesel, Benzin DI und Gasfahrzeugen”, contract no 15.0002.PJ/N375-0396.

References

[1] Mathis U, Mohr M, Forss A. Comprehensive particle characterization of modern gasoline and diesel passenger cars at low ambient temperatures. Atmos Environ 2005;39(1):107–17. https://doi.org/10.1016/j.atmosenv.2004.09.029.
[2] Schreiber D, Forss A-M, Mohr M, Dimopoulos P. Particle characterization of modern CNG, gasoline and diesel passenger cars. SAE Technical Paper 2007; 2007–24-0123.. https://doi.org/10.4271/2007-24-0123.
[3] Giechaskiel B, Martini G. Review on engine exhaust sub-23 nm solid particles. JRC Science and Policy Reports 2014;JRC90365, EUR 26653 EN. https://doi.org/10.2790/22597.
[4] Giechaskiel B, Manfredi U, Martini G. Engine exhaust solid Sub-23 nm Particles: I. Literature survey. SAE Int J Fuels Lubr 2014;7(3):950–64. https://doi.org/10.4271/2014-01-2834.
[5] Lee Z, Kim T, Park S. Influences of exhaust load and injection timing on particle number emissions in a gasoline direct injection engine. Fuel 2020;268:117344. https://doi.org/10.1016/j.fuel.2020.117344.
[6] Yu X, Guo Z, He L, Dong W, Sun P, Shi W, Du Y, He F. Effect of gasoline/n-butanol blends on gaseous and particle emissions from an SI direct injection engine. Fuel 2018;229:1–10. https://doi.org/10.1016/j.fuel.2018.05.003.
[7] Ko J, Kim K, Chung W, Myung C-L, Park S. Characteristics of on-road particle number (PN) emissions from a GDI vehicle depending on a catalytic stripper (CS) and a metal-foam gasoline particulate filter (GPF). Fuel 2019;238:363–74. https://doi.org/10.1016/j.fuel.2018.10.091.
[8] Alanen J, Saukko E, Lehtoranta K, Murtonen T, Timonen H, Hillamo R, Karjalainen P, Kuuluvainen H, Harra J, Keskinen J, Rönkkö T. The formation and physical properties of the particle emissions from a natural gas engine. Fuel 2015; 162:155–61. https://doi.org/10.1016/j.fuel.2015.09.003.
[9] Kittelson DB. Engines and nanoparticles. J Aerosol Sci 1998;29(5-6):575–88. https://doi.org/10.1016/S0021-8502(97)10037-4.
[10] Barone TL, Storey JME, Youngquist AD, Szybist JP. An analysis of direct-injection spark-ignition (DISI) soot morphology. Atmos Environ 2012;49:268–74. https://doi.org/10.1016/j.atmosenv.2011.11.047.
[11] Lapuerta M, Martos FJ, Herreros JM. Effect of engine operating conditions on the size of primary particles composing diesel soot agglomerates. J Aerosol Sci 2007;38 (4):455–66. https://doi.org/10.1016/j.jaerosci.2007.02.001.
[12] Liati A, Dimopoulos Eggenschwiler P. Characterization of particulate matter deposited in diesel particulate filters: Visual and analytical approach in macro-, micro- and nano-scales. Combustion Flame 2010;157(9):1658–70. https://doi.org/10.1016/j.combustflame.2010.02.015.
[13] Liati A, Dimopoulos Eggenschwiler P, Schreiber D, Zelenay V, Ammann M. Variations in diesel soot reactivity along the exhaust after-treatment system, based on the morphology and nanostructure of primary soot particles. Combustion Flame 2013;160(3):671–81. https://doi.org/10.1016/j.combustflame.2012.10.024.

[14] Liati A, Schreiber D, Dimopoulos Eggenschwiler P, Arroyo Rojas Dasilva Y, Spiteri AC. Electron microscopic characterization of soot particulate matter emitted by modern direct injection gasoline engines. Combustion Flame 2016;166:307–15. https://doi.org/10.1016/j.combustflame.2016.01.031.
[15] Gaddam CK, Vander Wal RL. Physical and chemical characterization of SIDI engine particulates. Combustion Flame 2013;160(11):2517–28. https://doi.org/10.1016/j.combustflame.2013.05.025.
[16] Liati A, Schreiber D, Arroyo Rojas Dasilva Y, Dimopoulos Eggenschwiler P. Ultrafine particle emissions from modern gasoline and diesel vehicles: An electron microscopic perspective. Environ Pollut 2018;239:661–9. https://doi.org/10.1016/j.envpol.2018.04.081.
[17] Giechaskiel B, Martini G. Engine Exhaust Solid Sub-23 nm Particles: II. Feasibility Study for PN Measurement Systems. SAE Technical Paper 2014;SAE2014-01-2832. https://doi.org/10.4271/2014-01-2832.
[18] Napolitano P, Alfè M, Guido C, Gargiulo V, Fraioli V, Beatrice C. Particle emissions from a HD SI gas engine fueled with LPG and CNG. Fuel 2020;269:117439. https://doi.org/10.1016/j.fuel.2020.117439.
[19] Giechaskiel B, Lähde T, Drossinos Y. Regulating particle number measurements from the tailpipe of light-duty vehicles: The next step? Environ Res 2019;172:1–9. https://doi.org/10.1016/j.envres.2019.02.006.
[20] Czerwinski J, Comte P, Engelmann D, Heeb N, Muñoz M, Bonsack P, Hensel V, Mayer A. PN-Emissions of Gasoline Cars MPI and Potentials of GPF, SAE Paper 2018; 2018-01-0363.
[21] Muñoz M, Haag R, Zeyer K, Mohn J, Comte P, Czerwinski J, Heeb NV. Effects of four prototype gasoline particle filters (GPFs) on nanoparticle and genotoxic pah emissions of a gasoline direct injection (GDI) vehicle. Environ Sci Technol 2018;52(18):10709–18.
[22] Zheng Z, Johnson KC, Liu Z, Durbin TD, Hu S, Huai T, Kittelson DB, Jung HS. Investigation of solid particle number measurement: Existence and nature of sub-23nm particles under PMP methodology. J Aerosol Sci 2011;42(12):883–97. https://doi.org/10.1016/j.jaerosci.2011.08.003.
[23] Ouf F-X, Sillon P. Charging efficiency of the electrical low pressure impactor's corona charger: Influence of the fractal morphology of nanoparticle aggregates and uncertainty analysis of experimental results. Aerosol Sci Technol 2009;43(7):685–98. https://doi.org/10.1080/02786820902878245.
[24] Liberda N, Pischinger S, Blessing J. Bestimmung des Liefergrades bei spülendem Ladungswechsel. Motortechnische Zeitschrift 2016:MTZ11/2016: 76-80.
[25] Klauer N, Zülch C, Schwarz C, Schünemann E. 2,0-L-Vierzylinder-Ottomotor von BMW mit Turboaufladung für SULEV. MTZ Motortech Z 2012;73(5):380–7.
[26] Dageförde H, Bertsch M, Kubach H, Koch T. Reduktion der Partikelemissionen bei Ottomotoren mit Direkteinspritzung. MTZ Motortech Z 2015;76(10):86–93.